

A two-dimensional model for slow convection at infinite Marangoni number

By A. THESS, D. SPIRN AND B. JÜTTNER

Institute for Fluid Mechanics, Dresden University of Technology, 01062 Dresden, Germany

(Received 14 May 1996 and in revised form 6 July 1996)

The free surface of a viscous fluid is a source of convective flow (Marangoni convection) if its surface tension is distributed non-uniformly. Such non-uniformity arises from the dependence of the surface tension on a scalar quantity, either surfactant concentration or temperature. The surface-tension-induced velocity redistributes the scalar forming a closed-loop interaction. It is shown that under the assumptions of (i) small Reynolds number and (ii) vanishing diffusivity this nonlinear process is described by a single self-consistent two-dimensional evolution equation for the scalar field at the free surface that can be derived from the three-dimensional basic equations without approximation. The formulation of this equation for a particular system requires only the knowledge of the closure law, which expresses the surface velocity as a linear functional of the active scalar at the free surface. We explicitly derive these closure laws for various systems with a planar non-deflecting surface and infinite horizontal extent, including an infinitely deep fluid, a fluid with finite depth, a rotating fluid, and an electrically conducting fluid under the influence of a magnetic field. For the canonical problem of an infinitely deep layer we demonstrate that the dynamics of singular (point-like) surfactant or temperature distributions can be further reduced to a system of ordinary differential equations, equivalent to point-vortex dynamics in two-dimensional perfect fluids. We further show, using numerical simulations, that the dynamical evolution of initially smooth scalar fields leads in general to a finite-time singularity. The present theory provides a rational framework for a simplified modelling of strongly nonlinear Marangoni convection in high-Prandtl-number fluids or systems with high Schmidt number.

1. Introduction

The description of flows driven or modified by surface tension gradients requires, in general, the solution of the full three-dimensional nonlinear equations of free-surface hydrodynamics (Levich 1962; Edwards, Brenner & Wasan 1991). Such a solution is often quite expensive computationally. Consequently it is tempting to ask whether the excursion into the third dimension can be simplified or avoided. This becomes even more attractive if one is interested in a self-consistent theory containing only free-surface quantities, as is the case in various problems of chemical engineering involving surfactants. Such an approach, based on boundary-integral techniques (Pozrikidis 1992), has recently proved useful for a similar problem, namely the description of monolayer domains at the air–water interface (Lubensky & Goldstein 1996).

The aim of the present paper is to demonstrate that under suitable assumptions the three-dimensional dynamics of surface-tension-driven flows can be mapped onto a

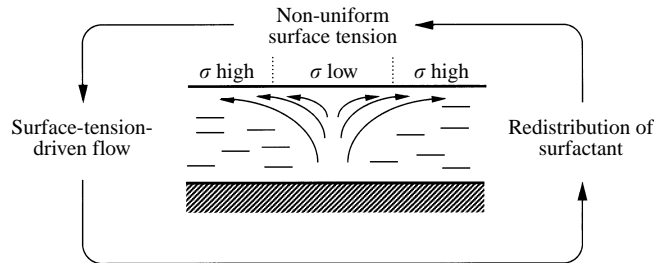


FIGURE 1. Schematic of the closed-loop interaction in Marangoni convection: A flow is created in a viscous fluid owing to non-uniform distribution of surface tension. The surface-tension-driven flow redistributes the surface tension.

self-consistent two-dimensional evolution equation for free-surface quantities. Before engaging in a systematic treatment of this problem, we wish to provide the reader with an intuitive understanding of the physical mechanisms involved.

The basic ingredients of surface-tension-driven convection, often called Marangoni convection (MC), are sketched in figure 1. An indispensable prerequisite for MC is the dependence of the surface tension σ on a scalar field θ which can be the temperature, concentration or a combination of both, henceforth referred to as the surfactant. We consider a situation in which the equation of state $\sigma(\theta)$ is well approximated by the linear relationship

$$\sigma = \sigma_0 - \gamma(\theta - \theta_0) \quad (1.1)$$

where σ_0 is the surface tension at a reference surfactant concentration θ_0 and γ the usually positive coefficient of surface tension variation. Although there are instances in which this relation is inappropriate (see e.g. Oron & Rosenau 1994), the majority of phenomena in MC can be understood in the framework of this simple relation.

As illustrated in figure 1, a non-uniform distribution of surface tension, resulting from non-uniformities of the surfactant concentration, induces a flow in the underlying fluid (Landau & Lifshitz 1987). This flow leads to a reordering of the surfactant distribution and thus to a reordering of the driving surface-forces, the latter process being governed by an advection–diffusion equation. The nonlinear character of this closed-loop interaction is best appreciated by considering the advection–diffusion equation

$$\partial_t \theta + \nabla \cdot (\mathbf{v}\theta) = D\nabla^2 \theta \quad (1.2)$$

describing the evolution of an insoluble surfactant, i.e. a surfactant residing entirely at the planar free surface of a fluid (Edwards *et al.* 1991). Here $\nabla = \mathbf{e}_x \partial_x + \mathbf{e}_y \partial_y$ and $\nabla^2 = \partial_x^2 + \partial_y^2$ denote the two-dimensional gradient and Laplacian, respectively, and D is the surface diffusion coefficient. Since the flow is driven entirely at the free surface, the surface velocity \mathbf{v} is a functional of the surfactant concentration, and (1.2) represents, at least in the formal sense, a self-consistent nonlinear evolution equation for the surfactant concentration. Unfortunately, it is a formidable task to extract useful information about the non-local functional $\mathbf{v}[\theta]$ from the full nonlinear Navier–Stokes equation. It is therefore the goal of the present paper to isolate such cases in which the Navier–Stokes equation can be approximated by the linear Stokes equation and the functional $\mathbf{v}[\theta]$ can be computed explicitly.

The concept of self-consistent two-dimensional Marangoni convection, exemplified by (1.2), is attractive for two reasons. On the one hand, it permits to the greatest possible extent the separation of the interfacial aspects of MC from those determined

by the hydrodynamics of the bulk flow. It thereby provides a useful vehicle for elucidating complex situations like surface-tension-driven Bénard convection (Davis 1987; Koschmieder 1993), thermocapillary migration of drops and bubbles (Oliver & De Witt 1994), free-surface turbulence in the presence of surfactants (Ting & Yue 1995; Sarpkaya 1996) as well as spreading of surfactants (Jensen 1995; Jensen & Grotberg 1992, 1993) in which such separation is not rigorously possible. On the other hand, the model (1.2) (possibly with a vector-valued function $\theta = (\theta_1, \theta_2, \dots, \theta_n)$ describing n concentration fields) represents a new class of mathematical models for pattern formation and frontogenesis in nonlinear systems where different closure laws $\mathbf{v}[\theta]$ can be ‘plugged in’ depending on the specific physical situation. From the conceptual point of view, the family of advection–diffusion equations (1.2) is a natural counterpart to the family of reaction–diffusion equations

$$\partial_t \theta = D \nabla^2 \theta + f(\theta) \tag{1.3}$$

(again with the vector $\theta = (\theta_1, \theta_2, \dots, \theta_n)$ representing the concentration of n species) widely considered as a prototype for pattern formation in nonlinear extended systems. The relation $\mathbf{v}[\theta]$, specifying the particular system, plays an analogous role in closing (1.2) as does the relation $f(\theta)$ for (1.3) specifying the reaction kinetics (Turing 1952).

The present paper is organized as follows. In §2 we formulate the basic ideas of the present theory and apply them in §3 to the simplest non-trivial problem, an infinitely deep layer. We demonstrate for this case that the dynamics of the system can be further reduced to a set of coupled nonlinear ordinary differential equations if one considers the evolution of singular surfactant distributions in the form of delta-functions, similar to point-vortex systems in two-dimensional ideal hydrodynamics. Moreover, we demonstrate numerically that the dynamical evolution of smooth initial data leads to a finite-time singularity. In §§4, 5 and 6 we generalize the canonical problem to a fluid with finite depth, a rotating fluid, and an electrically conducting fluid under the influence of a magnetic field, respectively. In §7 we summarize our results and discuss possible extensions of our work.

2. Basic concepts

Consider a viscous fluid bounded by a planar non-deflecting free surface $z = 0$ with infinite horizontal extent. The fluid is characterized by its kinematic viscosity ν , density ρ , dynamic viscosity $\mu = \rho\nu$, and by the coefficient γ of surface tension variation defined in (1.1). In what follows all quantities at the free surface will be denoted by lower-case letters, while upper-case letters will be used to denote the values of physical quantities in the volume. Moreover, $\tilde{\nabla}$ and ∇ will denote the three-dimensional and two-dimensional Nabla operators, respectively.

Let a scalar field Θ be immersed in the fluid, which modifies the surface tension according to (1.1), and let us denote by θ the value of the scalar at the free surface. The field Θ referred to as the surfactant, encapsulates three important particular cases, namely the case of the concentration of a completely soluble surfactant $\Theta = C(x, y, z, t)$ with constant mass $\int C d^3 \mathbf{x}$, the case of an insoluble surfactant $\theta = c_s(x, y, t)$ residing at the free surface and having again constant mass $\int c_s d^2 \mathbf{x}$, and finally the case of a temperature field $\Theta = T(x, y, z, t)$ which, in the absence of heat sources obeys $\int T d^3 \mathbf{x} = \text{const}$.

The dynamics of the completely soluble surfactant Θ in a velocity field \mathbf{V} is governed by the three-dimensional advection–diffusion equation

$$\partial_t \Theta + \tilde{\nabla} \cdot (\mathbf{V} \Theta) = D \tilde{\nabla}^2 \Theta, \tag{2.1}$$

where D denotes the diffusivity. In the thermal case, D has to be replaced by the thermal diffusivity κ . The evolution of an insoluble surfactant θ , confined to the free surface, is described by the two-dimensional equation

$$\partial_t \theta + \nabla \cdot (\mathbf{v}\theta) = D_s \nabla^2 \theta, \quad (2.2)$$

where D_s is called the surface diffusivity.

It should be noted that (2.1) and (2.2) represent only two particular cases of the general surfactant dynamics which is characterized by the presence of both a three-dimensional bulk concentration $C(\mathbf{X}, t)$ and an excess surface concentration $c_s(\mathbf{x}, t)$. While the dynamics of the former is described by the equation $\partial_t C + \tilde{\nabla} \cdot (\mathbf{V}C) = D\tilde{\nabla}^2 C$, identical to (2.1), the behaviour of the latter is governed by the generalized version $\partial_t c_s + \nabla \cdot (\mathbf{v}c_s) = D_s \nabla^2 c_s + J(c_s, c)$ of (2.2). The source term J , for which various models exist in literature, describes the exchange of surfactant concentration between the surface and the bulk and depends on the value c of the bulk concentration at the free surface. The particular case of an insoluble surfactant comes from $C \equiv 0$ and $J \equiv 0$, while the opposite case of a complete solubility corresponds to $c_s = 0$. We will show in §7 that the theory formulated below can be extended to any non-trivial transport relation J with the proviso that D has to be zero.

As illustrated in figure 1, the velocity field is determined by the free-surface surfactant concentration through the three-dimensional incompressible Navier–Stokes equation

$$\partial_t \mathbf{V} + (\mathbf{V} \cdot \tilde{\nabla})\mathbf{V} = -\tilde{\nabla}P + \nu \tilde{\nabla}^2 \mathbf{V} + \mathbf{F}, \quad (2.3)$$

$$\tilde{\nabla} \cdot \mathbf{V} = 0, \quad (2.4)$$

subject to the boundary conditions

$$\mu \partial_z V_x = -\gamma \partial_x \theta, \quad \mu \partial_z V_y = -\gamma \partial_y \theta, \quad V_z = 0 \quad \text{at } z = 0 \quad (2.5)$$

and to appropriate conditions at the lower boundary. The force term in the Navier–Stokes equation, to be specified later, will either represent the Coriolis force in the rotating fluid of §5 or the Lorentz force in the electrically conducting fluid of §6, arising from the interaction of the fluid with an applied homogeneous magnetic field. The term \mathbf{F} does not contain any external forcing and is thereby purely dissipative. In fact, the motion of the fluid is exclusively produced by the first two Marangoni boundary conditions (2.5) which express the continuity of the tangential stress across the free surface (cf. Landau & Lifshitz 1987; Davis 1987). These boundary conditions provide the feedback between the scalar and the flow field. It is important to emphasize once more that the entire three-dimensional flow \mathbf{V} is determined by the two-dimensional surfactant concentration θ at the free surface. In order to formulate the conditions under which the basic equations (2.1)–(2.5) can be simplified, we have to consider the values of the relevant non-dimensional numbers, which are in our case the Reynolds number and the Péclet number.

Let $\Delta\theta$ denote a variation of surfactant concentration over the lengthscale ℓ , and $\Delta\sigma = \gamma\Delta\theta$ the associated surface tension variation. Then the boundary condition (2.5) provides the estimate

$$v \sim \frac{\Delta\sigma}{\mu} \quad (2.6)$$

for the magnitude of the induced velocity. The Reynolds number $Re = v\ell/\nu$ and the Péclet, or Marangoni, number $Pe = v\ell/D$ (or $Pe = v\ell/\kappa$ in the thermal case) can

then be estimated as

$$Re = \frac{\Delta\sigma\ell}{\mu v}, \quad (2.7)$$

$$Pe = \frac{\Delta\sigma\ell}{\mu D}. \quad (2.8)$$

While the Reynolds number is a dimensionless measure of the importance of convective transport of momentum in relation to diffusive transport, the Péclet number measures the ratio between convective and diffusive transport of the surfactant.

Let us estimate the order of magnitude of these parameters for a typical example where a surfactant, namely sodium dodecyl sulfate at 10 % of its critical micelle concentration, acts on a silicone oil–water interface (Park, Maruvada & Yoon 1994). With $\Delta\sigma \sim 7 \times 10^{-3} \text{ kg s}^{-2}$ and $\mu \sim 10^{-1} \text{ kg ms}^{-1}$ we can estimate the characteristic velocity as $v \sim 7 \times 10^{-2} \text{ m s}^{-1}$. Considering small-scale fluctuations over the lengthscale $\ell \sim 10^{-3} \text{ m}$ and using $D \sim 10^{-8} \text{ m}^2 \text{ s}^{-1}$ for the surface diffusion coefficient of the surfactant (De Wit, Gallez & Christov 1994) we obtain the estimates

$$Re \sim 7 \times 10^{-2}, \quad (2.9)$$

$$Pe \sim 7 \times 10^3. \quad (2.10)$$

$Re \ll 1$ shows the dominance of the diffusive momentum transport over advection, whereas $Pe \gg 1$ suggests the overwhelming importance of convective surfactant transport in comparison with diffusion. Conditions similar to (2.9) and (2.10) are encountered in a wide class of surface-tension-driven flows, including Bénard convection at high Marangoni number (Nitschke & Thess 1995), adsorption controlled Marangoni flow past emulsion droplets (Edwards *et al.* 1991, chap. 5.6), evaporative convection (Berg, Acrivos & Boudart 1966) and thermocapillary migration of drops and bubbles (Oliver & De Witt 1994). Even in cases where the integral Reynolds number is not small, for instance high-Marangoni-number convection near lateral walls (Cowley & Davis 1983; Zebib, Homsy & Meiburg 1985) or interaction between vortices and a surfactant-contaminated free surface (Tsai & Yue 1995; Tryggvason *et al.* 1992), the condition $Re \ll 1$ is fulfilled for surfactant fluctuations on scales smaller than the thickness of the viscous boundary layer. The smallness of the Reynolds number demonstrates the fact that the (linear) Stokes equation

$$-\tilde{\nabla}P + \nu\tilde{\nabla}^2V + \mathbf{F} = 0 \quad (2.11)$$

can be used to approximate the flow instead of the (nonlinear) Navier–Stokes equation (2.3).

Progress in hydrodynamics is often aided by considering fluids with vanishing molecular transport coefficients. With the condition $Pe \gg 1$ in mind, we shall therefore assume that the diffusivity of the surfactant is zero ($D = 0$ in (2.1) or (2.2)). This assumption ensures that the evolution of θ is only a redistribution of the initial two-dimensional distribution by the two-dimensional surface velocity \mathbf{v} with no ‘exchange of information’ between the surface concentration and the bulk concentration. Indeed, a particle initially located at the free surface cannot leave the free surface on account of the third boundary condition in (2.5), and cannot exchange concentration with adjacent particles owing to the absence of diffusion. As a result, equations (2.1) and (2.2) at the free surface can be written as

$$\partial_t\theta + (\mathbf{v} \cdot \nabla)\theta = 0, \quad (2.12)$$

for the soluble surfactant, and

$$\partial_t \theta + \nabla \cdot (\mathbf{v}\theta) = 0, \quad (2.13)$$

for the insoluble surfactant. The first equation is derived by evaluating (2.1) at the free surface and making use of the third boundary condition (2.5). Notice that (2.12) and (2.13) are different since the divergence of the surface velocity $\nabla \cdot \mathbf{v} = \partial_x v_x + \partial_y v_y = -\partial_z v_z$ is non-zero. For a soluble surfactant, θ is conserved along the trajectory of each particle but the integral quantity $\int \theta d^2x$ is generally not constant. For an insoluble surfactant, θ can change along a Lagrangian trajectory but $\int \theta d^2x$ is conserved. Both equations (2.12) and (2.13) contain only free surface quantities. Strictly speaking, the zero-diffusivity assumption is only necessary for the soluble surfactant; the insoluble surfactant equation is of self-consistent form even in the presence of diffusion. For the sake of uniformity, however, we adopt the condition $D = 0$ for both models.

Equations (2.12) and (2.13) do not represent a self-consistent *closed* system until we are able to specify the ‘closure law’ $\mathbf{v}[\theta]$, expressing the surface velocity as a functional of the surfactant concentration. As a result of our assumption $Re \ll 1$ this can be done explicitly, since the relation between surfactant concentration and velocity is given by the linear Stokes problem. We shall use a method based on Fourier-transforms for the derivation of the closure laws rather than boundary-integral techniques (Jansons & Lister 1988; Pozrikidis 1992) because the former can be more easily generalized to the rotating and magnetic cases and because it can be easily implemented numerically using pseudospectral methods. Introducing the Fourier-transformed quantities $\hat{\theta}$, $\hat{\mathbf{V}}$, and $\hat{\boldsymbol{\Omega}} = i\mathbf{k} \times \hat{\mathbf{V}}$ through

$$\theta(\mathbf{x}) = \frac{1}{4\pi^2} \int \hat{\theta}(\mathbf{k}) e^{i\mathbf{k}\cdot\mathbf{x}} d^2\mathbf{k}, \quad (2.14)$$

$$\mathbf{V}(\mathbf{X}) = \frac{1}{4\pi^2} \int \hat{\mathbf{V}}(\mathbf{k}, z) e^{i\mathbf{k}\cdot\mathbf{x}} d^2\mathbf{k}, \quad (2.15)$$

with the two-dimensional wavenumber $\mathbf{k} = k_x \mathbf{e}_x + k_y \mathbf{e}_y$ and $k = (k_x^2 + k_y^2)^{1/2}$ we can transform the Stokes problem (2.4), (2.5) and (2.11) into

$$v(D^2 - k^2)\hat{\Omega}_z + i(k_x \hat{F}_y - k_y \hat{F}_x) = 0, \quad (2.16)$$

$$v(D^2 - k^2)^2 \hat{V}_z - (ik_x D \hat{F}_x + ik_y D \hat{F}_y + k^2 \hat{F}_z) = 0. \quad (2.17)$$

The free-surface boundary conditions can be converted into

$$-\mu D^2 \hat{V}_z = \gamma k^2 \hat{\theta}, \quad \hat{V}_z = 0, \quad D \hat{\Omega}_z = 0, \quad (2.18)$$

where $D = d/dz$. Equation (2.16) [(2.17)] follows from the Stokes equation by taking the curl of (2.11) once [twice] and by evaluating the z -component. The first boundary condition in (2.18) is obtained by adding the x -derivative of the first boundary condition in (2.5) to the y -derivative of the second boundary condition in (2.5) and making use of the incompressibility constraint. Finally, the third boundary condition in (2.18) follows from the identity $D\Omega_z = -\partial_x \Omega_x - \partial_y \Omega_y$ together with the relations $\Omega_x = (\gamma/\mu)\partial_y \theta$ and $\Omega_y = -(\gamma/\mu)\partial_x \theta$, the latter being a consequence of (2.5) and $V_z = 0$. Once the type of force $\mathbf{F}[\mathbf{v}]$ is specified, the vertical velocity and vertical vorticity as obtained from (2.16)–(2.18) determine the entire flow field as

$$\hat{V}_x = \frac{ik_x}{k^2} D \hat{V}_z + \frac{ik_y}{k^2} \hat{\Omega}_z, \quad (2.19)$$

$$\hat{V}_y = \frac{ik_y}{k^2} D\hat{V}_z - \frac{ik_x}{k^2} \hat{\Omega}_z, \tag{2.20}$$

(cf. Chandrasekhar 1961).

Since the Stokes problem (2.16)–(2.18) is linear, both $D\hat{V}_z$ and $\hat{\Omega}_z$ necessary to evaluate the free surface velocity are linear functions of $\hat{\theta}$. If the force in (2.11) is homogeneous and isotropic in the (x, y) -plane, we can, therefore, without loss of generality, write equations (2.19) and (2.20) at the free surface as

$$\hat{\mathbf{v}} = -i\mathbf{k}\gamma_{\parallel}(k)\hat{\theta} + i\mathbf{k}_{\perp}\gamma_{\perp}(k)\hat{\theta} \tag{2.21}$$

(with $\mathbf{k}_{\perp} = \mathbf{e}_x k_y - \mathbf{e}_y k_x$) where the closure functions γ_{\parallel} and γ_{\perp} are defined as

$$\gamma_{\parallel}(k) = -\frac{D\hat{V}_z(k, 0)}{k^2\hat{\theta}}, \tag{2.22}$$

$$\gamma_{\perp}(k) = +\frac{\hat{\Omega}_z(k, 0)}{k^2\hat{\theta}}. \tag{2.23}$$

The physical meaning of the closure functions, which are the main focus of the present work, becomes clear by considering the surface velocity induced by a single Fourier mode $\theta = \cos(kx)$. Using (2.21) the velocity field is easily determined as

$$\mathbf{v} = [\gamma_{\parallel}(k)\mathbf{e}_x + \gamma_{\perp}(k)\mathbf{e}_y] k \sin(kx). \tag{2.24}$$

Thus, γ_{\parallel} and γ_{\perp} measure the longitudinal and transverse velocity component induced by a unidirectional surfactant distribution. If γ_{\parallel} and γ_{\perp} were independent of the wavenumber k , we would have

$$\mathbf{v} = -\gamma_{\parallel}\nabla\theta - \gamma_{\perp}\nabla_{\perp}\theta, \tag{2.25}$$

where $\nabla_{\perp} = \mathbf{e}_z \times \nabla$. Once the closure functions γ_{\parallel} and γ_{\perp} are determined by solving the Stokes equations for a specific problem, equation (2.12) [or (2.13)] together with (2.21) become a closed set. The rest of the paper is devoted to the determination of closure laws for specific physical systems.

Before proceeding to the next section, however, a comment is in order on possible deformations of the free surface. The present theory is developed for a non-deflecting planar surface. At first glance, this assumption may seem to lack physical justification because any fluid motion is accompanied by a deformation of the free surface. The validity of such an assumption, discussed in depth by Scriven & Sternling (1964) and Davis (1987) is a subtle question that has to be considered separately for each specific problem. In the absence of gravity, the non-dimensional surface deflection $h(x, y)/\ell$ is of the order of the dynamic Bond number $\Delta\sigma/\sigma_0$ which is usually much smaller than unity. However, there are instances such as pulmonary fluid dynamics (Grotberg 1994; Jensen & Grotberg 1992) and marine hydrodynamics (Sarpkaya 1996) in which consideration of surface deflections is crucial.

3. The canonical problem: semi-infinite layer

3.1. Closure law

The simplest application of the basic ideas sketched in the previous section pertains to a layer with infinite depth, i.e. $z < 0$, and no volume force ($\mathbf{F} = 0$ in (2.11)). Measuring space, time, wavenumber, and surfactant concentration in units of ℓ , $\mu\ell/\Delta\sigma$, $1/\ell$, and $\Delta\theta$ where ℓ is the scale of variation of surfactant concentration, and

introducing the non-dimensional quantities $W(z)$ and $H(z)$ via

$$\hat{V}_z = \frac{\Delta\sigma}{\mu} W, \quad \hat{\Omega}_z = \frac{\Delta\sigma}{\mu\ell} H, \quad (3.1)$$

the Stokes problem for the semi-infinite layer becomes

$$(\mathbf{D}^2 - k^2)^2 W = 0, \quad (3.2)$$

$$(\mathbf{D}^2 - k^2)H = 0. \quad (3.3)$$

The boundary conditions at the free surface $z = 0$ are

$$\mathbf{D}^2 W = -k^2 \hat{\theta}, \quad W = 0, \quad \mathbf{D}H = 0, \quad (3.4)$$

while at infinity we require

$$W \rightarrow 0, \quad H \rightarrow 0. \quad (3.5)$$

Notice that there is no coupling between the vertical velocity W and the vertical vorticity H . Therefore, the solution to the Stokes problem (3.2)–(3.5) can be easily found as

$$W = -kz \frac{1}{2} \hat{\theta} e^{kz} \quad (3.6)$$

$$H = 0 \quad (3.7)$$

Using the definitions (2.22) and (2.23) we can readily derive the closure law

$$\gamma_{\parallel} = \frac{1}{2k}, \quad \gamma_{\perp} = 0, \quad (3.8)$$

or, in other words,

$$\hat{\mathbf{v}} = -\frac{i\mathbf{k}}{2k} \hat{\theta}. \quad (3.9)$$

This relation, in conjunction with (2.12) for a soluble surfactant or with (2.13) for an insoluble surfactant, forms a self-consistent two-dimensional system for the surfactant concentration. Notice that its derivation from the three-dimensional non-diffusive problem (2.1), (2.2), (2.4), (2.5) and (2.11) did not involve any approximation.

The closure law for the semi-infinite layer (3.9) can be transformed back to physical space for both one-dimensional and two-dimensional surfactant distributions.

In the one-dimensional case $\hat{\mathbf{v}} = \hat{v} \mathbf{e}_x$ and $\mathbf{k} = k \mathbf{e}_x$ so that (3.9) becomes

$$\hat{v} = -\frac{1}{2} i \operatorname{sign}(k) \hat{\theta}, \quad (3.10)$$

with $\operatorname{sign}(k) = +1$ for $k > 0$ and $\operatorname{sign}(k) = -1$ for $k < 0$. Transformation of the result back to physical space yields

$$v(x) = -\frac{i}{4\pi} \int_{-\infty}^{\infty} \operatorname{sign}(k) \hat{\theta}(k) e^{ikx} dk. \quad (3.11)$$

With the help of the integral representations

$$\operatorname{sign}(k) = \frac{1}{2\pi i} \int_{-\infty}^{\infty} \frac{e^{ikx} - e^{-ikx}}{x} dx \quad (3.12)$$

$\theta(x)$	$v(x)$
$\cos(kx)$	$\frac{1}{2} \sin(kx)$
$\frac{1}{x^2 + a^2}$	$\frac{x}{2a(x^2 + a^2)}$
$\frac{x}{x^2 + a^2}$	$-\frac{a}{2(x^2 + a^2)}$
$\log \left \frac{a-x}{x-b} \right \quad (a < b)$	$0 \quad (-\infty < x < a)$ $\frac{1}{2}\pi \quad (a < x < b)$ $0 \quad (b < x < \infty)$

TABLE 1. Examples of the relation between the surface velocity and surfactant concentration in the one-dimensional case for a semi-infinite layer. The relations correspond to equation (3.14).

and

$$\delta(x) = \frac{1}{2\pi} \int_{-\infty}^{\infty} e^{ikx} dk, \tag{3.13}$$

we derive the desired relation

$$v(x) = -\frac{1}{2\pi} \int_{-\infty}^{\infty} \frac{\theta(x')}{x' - x} dx' \tag{3.14}$$

expressing, in dimensionless form, the one-dimensional velocity field created by the one-dimensional surfactant distribution $\theta(x)$. This relation can be written in terms of the Hilbert transform \mathcal{H} (Erdélyi 1954) as

$$v = -\frac{1}{2} \mathcal{H} \theta. \tag{3.15}$$

It is important to emphasize that the surface velocity is related to the surfactant concentration by a non-local operator, or more precisely, by a singular integral operator of homogeneity degree zero. The latter statement implies $\mathcal{H}(\lambda x) = \mathcal{H}(x)$ which is the mathematical manifestation of the fact that the semi-infinite layer does not possess any characteristic lengthscale.

Equation (3.15) furnishes a variety of exact kinematic relations between surfactant concentration and surface velocity. For example, the concentration field $\theta(x) = \delta(x)$, which corresponds to an infinitely thin line of excess surfactant concentration, creates the surface velocity

$$v(x) = \frac{1}{2\pi x} \tag{3.16}$$

which decreases as the inverse distance from the line. For more illustrations of the closure law the reader may consult the variety of Hilbert transforms tabulated by Erdélyi (1954). Table 1 summarizes a few of them. As table 1 shows, the Hilbert transform of a trigonometric function differs from its derivative only by the lack of the wavenumber. Roughly speaking, the Hilbert transform is a smoother operator than the derivative.

Physical intuition seems to suggest that the surface velocity in Marangoni convection is proportional to the gradient of surfactant concentration or surface temperature. The fourth relation in table 1 provides a counterexample showing that the surface

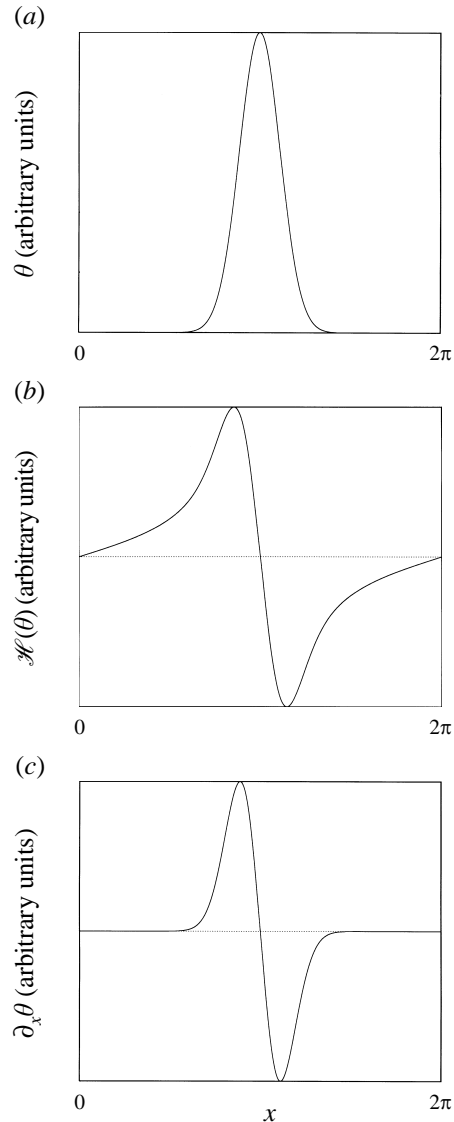


FIGURE 2. Illustration of the non-local relationship between (a) the surfactant concentration θ and (b) the induced velocity $v \sim -\mathcal{H}(\theta)$. The first derivative of θ , a local operation, is shown in (c) for comparison. Periodic boundary conditions are used.

velocity may vanish in regions of non-zero gradient of surfactant concentration. Observe that $v_x = 0$ for $x < a$ and $x > b$ is not in contradiction with the boundary conditions (2.5). The latter requires non-zero shear $\partial_z V_x(x, 0)$ but does not impose any constraints on the surface velocity itself. Example 4 from table 1 does not however represent the generic case since the temperature field is singular. Figure 2 demonstrates another aspect of this non-local $\theta - v$ relation. The plots, including a periodic function with Gaussian shape (figure 2a) together with its Hilbert transform (figure 2b) and its first derivative (figure 2c), show that the velocity (proportional to the Hilbert transform) may well be non-zero in regions where the gradient vanishes.

In the two-dimensional case, the closure law (3.9) is most conveniently translated into physical space by introducing a velocity potential ϕ via

$$\mathbf{v} = -\nabla\phi, \tag{3.17}$$

and solving the resulting equation

$$\Delta^{1/2}\phi = \frac{1}{2}\theta \tag{3.18}$$

using the Green's function of the operator $\Delta^{1/2}$. The latter is defined as a multiplication in Fourier space with the modulus of the wavenumber, i.e. $\widehat{\Delta^{1/2}\phi} = k\hat{\phi}$. The Green's function of this operator, defined by $\Delta^{1/2}G = \delta(\mathbf{x})$ is calculated by applying the inverse Fourier transform to $1/k$ and by making use of the auxiliary relation

$$\hat{k}^\alpha = \frac{2^\alpha \Gamma \frac{1}{2}(n + \alpha)}{\pi^{-n/2} \Gamma(-\frac{1}{2}\alpha)} x^{-(n+\alpha)} \tag{3.19}$$

(Helgasson 1980) where n is the dimension of the space, and Γ the gamma function. The result for $\alpha = -1$ and $n = 2$

$$G(\mathbf{x}) = \frac{1}{2\pi|\mathbf{x}|} \tag{3.20}$$

provides the integral representation

$$\phi(\mathbf{x}) = \frac{1}{4\pi} \int \frac{\theta(\mathbf{x}')}{|\mathbf{x} - \mathbf{x}'|} d^2\mathbf{x}' \tag{3.21}$$

for the velocity potential from which we derive the final result for the two-dimensional surface velocity as

$$\mathbf{v}(\mathbf{x}) = \frac{1}{4\pi} \int \frac{\mathbf{x} - \mathbf{x}'}{|\mathbf{x} - \mathbf{x}'|^3} \theta(\mathbf{x}') d^2\mathbf{x}' \tag{3.22}$$

in terms of the surfactant concentration. Equation (3.22) immediately furnishes the radial velocity caused by a point-like spot of surfactant $\theta(\mathbf{x}) = \delta(\mathbf{x} - \mathbf{x}_0)$ as

$$v_r = \frac{1}{4\pi r^2} \tag{3.23}$$

where $r = |\mathbf{x} - \mathbf{x}_0|$. This relation implies that the flux $2\pi r v_r$ through a circle around \mathbf{x}_0 with radius r decays as $(2r)^{-1}$.

3.2. Dynamics of singular surfactant distributions: the one-dimensional case

So far we have determined the kinematically possible velocity fields belonging to a given surfactant concentration field. In this section we wish to elucidate the dynamical consequences of the velocity for the redistribution of a soluble surfactant. The simplest way of accomplishing this task is to consider the dynamics of one-dimensional singular surfactant distributions in the form of N infinitely thin lines located at the positions $x_n(t)$, to be determined from the governing equations. In the theory of two-dimensional perfect fluids such an approach is called point-vortex dynamics (Aref 1983). In our case, the singular surfactant distribution plays an analogous role to that of point vortices in two-dimensional fluid dynamics.

Consider N infinitely thin lines of surfactant concentration with strength θ_n located at the positions x_n ($n = 1, \dots, N$). Then

$$\theta(x) = \sum_{n=1}^N \theta_n \delta(x - x_n). \quad (3.24)$$

Notice that a single line represents a weak stationary solution of (2.12) with (3.19) inducing the velocity field

$$v_n(x) = \frac{1}{2\pi} \frac{\theta_n}{x - x_n}. \quad (3.25)$$

As a result, the dynamical state of the system is uniquely characterized by the time-dependent positions $x_n(t)$. To derive the evolution equation for these quantities we observe that the n th line is advected by the velocity field created by the $(N - 1)$ other lines. Since the Stokes problem is linear, the velocity experienced by the n th line is simply the superposition of the velocity fields created by all other lines. This is mathematically expressed as

$$\frac{dx_n}{dt} = \frac{1}{2\pi} \sum_{m=1, m \neq n}^N \frac{\theta_m}{x_n - x_m}. \quad (3.26)$$

This system represents a closed set of nonlinear ordinary differential equations for the positions $x_n(t)$ of the lines with non-zero surfactant concentration. As in point-vortex dynamics of ideal fluids, we have thereby reduced the continuous problem to a finite-dimensional one.

While a systematic investigation of (3.26) is not undertaken here, we mention three particular cases in which (3.26) can be solved in a straightforward manner. To this end we first consider the evolution of two lines with positive surfactant concentration $\theta_1 = \theta_2 = 1$ located at x_1 and x_2 (with $x_2 > x_1$) which is described by

$$\frac{dx_1}{dt} = \frac{1}{2\pi(x_1 - x_2)}, \quad \frac{dx_2}{dt} = \frac{1}{2\pi(x_2 - x_1)}. \quad (3.27)$$

By introducing the centroid position $\rho = x_1 + x_2$ and the distance $r = x_2 - x_1$ we can reformulate these two equations as

$$\frac{d\rho}{dt} = 0, \quad \frac{dr}{dt} = \frac{1}{\pi r}. \quad (3.28)$$

Denoting the initial conditions by $\rho = \rho_0$ and $r = r_0$, one obtains the solutions

$$\rho = \rho_0, \quad r(t) = r_0 \left(1 + \frac{2t}{\pi r_0^2} \right)^{1/2}. \quad (3.29)$$

This solution describes two lines of positive surfactant concentration repelling each other. For large times, the distance between them increases as $t^{1/2}$. The second example involves two negative lines with $\theta_1 = \theta_2 = -1$. Using the same procedure as in the previous example, we readily obtain the solution

$$\rho = \rho_0, \quad r(t) = r_0 \left(1 - \frac{2t}{\pi r_0^2} \right)^{1/2}, \quad (3.30)$$

which describes the approach of two lines with negative surfactant concentration and their collapse after finite time $\tau = \frac{1}{2}\pi r_0^2$. Our final example involves two opposite lines,

i.e. $\theta_1 = +1$, $\theta_2 = -1$ for which we find

$$\rho(t) = \rho_0 + \frac{t}{2\pi r_0}, \quad r = r_0. \tag{3.31}$$

This solution describes two opposite lines translating from the positive to the negative concentration with constant speed and constant separation.

It is probable that the singular lines are prone to two-dimensional instabilities transforming them into curved objects. The description of their dynamics, however, would require more sophisticated methods, reminiscent of contour-dynamics in two-dimensional turbulence.

3.3. Dynamics of singular surfactant distributions: the two-dimensional case

Next we turn to the formulation of the two-dimensional ‘point-vortex equations’ in which the singular structures are point-like spots of surfactant distribution with strength θ_n . We assume θ to be of the form

$$\theta(x) = \sum_{n=1}^N \theta_n \delta(x - \mathbf{x}_n). \tag{3.32}$$

By (3.23) each spot creates the velocity

$$\mathbf{v}_n(x) = \frac{\theta_n}{4\pi} \frac{\mathbf{x} - \mathbf{x}_n}{|\mathbf{x} - \mathbf{x}_n|^3}. \tag{3.33}$$

Using the same arguments as before, we arrive at the two-dimensional analogue to (3.26)

$$\frac{d\mathbf{x}_n}{dt} = \frac{1}{4\pi} \sum_{m=1, m \neq n}^N \theta_m \frac{\mathbf{x}_n - \mathbf{x}_m}{|\mathbf{x}_n - \mathbf{x}_m|^3}, \tag{3.34}$$

which represents again a nonlinear system of ordinary differential equations for the positions $\mathbf{x}_n = x_n(t)\mathbf{e}_x + y_n(t)\mathbf{e}_y$ of the singular spots.

It is straightforward to work out the generalization of the three previous examples to the two-dimensional case. The two-dimensional analogue to (3.27) for positive like-sign spots $\theta_1 = \theta_2 = 1$ is

$$\frac{d\mathbf{x}_1}{dt} = \frac{1}{4\pi} \frac{\mathbf{x}_1 - \mathbf{x}_2}{|\mathbf{x}_1 - \mathbf{x}_2|^3}, \quad \frac{d\mathbf{x}_2}{dt} = \frac{1}{4\pi} \frac{\mathbf{x}_2 - \mathbf{x}_1}{|\mathbf{x}_2 - \mathbf{x}_1|^3}. \tag{3.35}$$

With the definitions $\boldsymbol{\rho} = \mathbf{x}_1 + \mathbf{x}_2$, $\mathbf{r} = \mathbf{x}_2 - \mathbf{x}_1$ and $r = |\mathbf{r}|$ we obtain

$$\frac{d\boldsymbol{\rho}}{dt} = 0, \quad \frac{d\mathbf{r}}{dt} = \frac{\mathbf{r}}{2\pi r^3}, \tag{3.36}$$

from which we derive the solution

$$\boldsymbol{\rho} = \boldsymbol{\rho}_0, \quad r(t) = r_0 \left(1 + \frac{3t}{2\pi r_0^3} \right)^{1/3}. \tag{3.37}$$

The distance between two positive spots increases as $r \sim t^{1/3}$, slower than in the one-dimensional case. The solution for the negative spots is found as

$$\boldsymbol{\rho} = \boldsymbol{\rho}_0, \quad r(t) = r_0 \left(1 - \frac{3t}{2\pi r_0^3} \right)^{1/3}, \tag{3.38}$$

which again collapses after the finite time $\tau = \frac{2}{3}\pi r_0^3$. Finally, two opposite spots with $\theta_1 = +1$, $\theta_2 = -1$ travel with constant speed $v = (\pi r_0^2)^{-1}$ as

$$\rho(t) = \rho_0 - \frac{r_0 t}{\pi r_0^3}, \quad r = r_0 \quad (3.39)$$

In perfect fluids, point vortex models are a powerful tool for investigating nonlinear vortex dynamics and approximating high-Reynolds-number two-dimensional turbulent flows with finite-dimensional systems. It seems therefore appropriate to use (3.26) and (3.34) for the investigation of elementary interaction processes in Marangoni convection in high-Schmidt-number problems or in high-Prandtl-number fluids.

3.4. Dynamics of smooth surfactant distributions: the one-dimensional case

After having formulated the evolution equations for singular surfactant distributions, we wish to provide some qualitative illustration of the generic dynamical evolution of this system starting from smooth initial data. Since a comprehensive analytical and numerical investigation of the dynamical evolution of specific cases is outside the scope of the present paper, we shall use the one-dimensional and two-dimensional dynamical evolution of a soluble surfactant as a prototype to provide an initial qualitative understanding of the nonlinear phenomena encountered. A preliminary report of this topic has been given by Thess, Spirn & Jüttner (1995).

In figure (3a) we plot the evolution of a soluble surfactant described by the one-dimensional equation

$$\partial_t \theta - (\mathcal{H}\theta)\partial_x \theta = 0, \quad (3.40)$$

which is equivalent to (2.12) with (3.9). We have rescaled the time as $t \rightarrow 2t$ in order to absorb the factor $\frac{1}{2}$ from the closure law (3.9). The solution is obtained using a pseudospectral method with 16 384 collocation points and periodic boundary conditions. For periodic boundary conditions, the Hilbert transform is evaluated in Fourier space by multiplying each Fourier component of θ with the sign of the wavenumber. It should be noted that the pseudospectral formulation is well suited for evaluating the non-local nonlinear term. The use of a finite-difference method with local mesh refinement, which might seem more appropriate to the resolution of the localized small-scale structure near $x = \pi$, does not offer any significant advantages in terms of computational efficiency. The grid points saved by using a localized mesh refinement, as opposed to the pseudospectral method, would be offset by a higher computational cost, $O(N^2)$ (N is the number of grid points), needed to evaluate $\mathcal{H}\theta$, whereas the pseudospectral method requires only $O[N \log(N)]$ operations. Therefore, the spectral formulation with equidistant grid points is approximately as efficient as a finite-difference method with local grid refinement.

Figure 3(a) shows that the region of high surfactant concentration (low surface tension) expands, while the region with low concentration in the vicinity of $x = \pi$ becomes compressed. After finite time $t_* \approx 1.275$, the first derivative (and all higher derivatives) diverge and the smooth solution ceases to exist. The formation of a finite-time singularity is common in many mathematical models of fluid-dynamical systems, including perfect fluids (Pumir & Siggia 1992; Grauer & Sideris 1995) Hele-Shaw flows (Goldstein, Pesci & Shelley 1995), geostrophic fronts (Constantin, Majda & Tabak 1994a, b) and free-surface flows (Eggers 1993; Kuznetsov, Spector & Zakharov 1994). The existence of a finite-time singularity, which can be proven rigorously for the complex version of (3.40) (Thess, Spirn & Jüttner 1995), is a signature of the strong tendency of the system to transfer energy towards smaller scales.

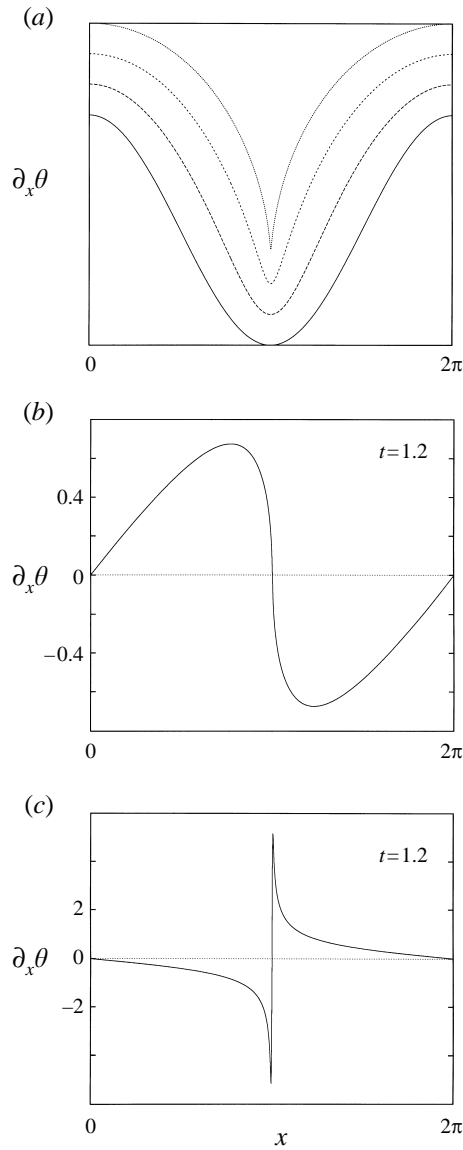


FIGURE 3. Finite-time singularity in surface-tension-driven flow. (a) Temporal evolution of surfactant concentration obtained from numerical solution of equation (3.40). Initial condition is $\theta = \cos(x)$, output is every $\Delta t = 0.4$, successive curves are shifted. (b,c) Surface velocity and first spatial derivative of surfactant concentration shortly before the singularity time $t_* = 1.275$.

The behaviour of the surface velocity $v \sim -\mathcal{H}\theta$ and of the first derivative $\partial_x \theta$ close to singularity time is plotted in figures 3(b) and 3(c), respectively. Although θ forms a cusp near $x = \pi$, the spatial structure of $v(x)$ remains remarkably smooth, which is a consequence of the non-local relation between θ and v . By contrast, $\partial_x \theta$ tends to develop sharp spikes whose height and width we found to scale with time, as respectively, $\max |\partial_x \theta| \sim \tau^{-3}$ and $\delta \sim \tau^2$, where $\tau = t_* - t$. This behaviour should be contrasted with $\max |\partial_x \theta| \sim \tau^{-1}$ and $\delta \sim \tau$ for the Burgers equation $\partial_t \theta - (\partial_x \theta)^2 = 0$. The qualitative nature of solutions to the Burgers equations is similar to that plotted

in figure (3a). The singularity of (3.40) is thus weaker than the singularity of the Burgers equation because $\max |\partial_x \theta|$ grows more quickly for the Burgers equation and because the speed of compression $d\delta/dt$ is constant for the Burgers equation while the speed of compression decreases for (3.40) as $d\delta/dt \sim -\tau$. The weakness of the singularity is due to the smoothness of the velocity field (figure 3b) compared to the function $\partial_x \theta$ (figure 3c). Numerical simulations with various initial conditions, including random initial conditions, have shown that close to the singularity, located at x_* and t_* , the surfactant distribution is of the self-similar form

$$\theta = \theta_* + \tau f\left(\frac{\xi}{\tau^2}\right), \quad (3.41)$$

where $\tau = t_* - t$, $\xi = x_* - x$, and θ_* denotes the value of the surfactant concentration at the bottom of the cusp. The function $f(\eta)$ with $\eta = \xi/\tau^2$ is found to have a quadratic minimum at $\eta = 0$ and scales as $f \sim \eta^{1/2}$ for large arguments. However, the numerical values of this function appear not to be universal. This can be understood by observing that the equation $f'(\mathcal{H}f - 2\eta) + f = 0$, obtained by inserting the similarity ansatz into (3.40) does not possess a global solution since $\mathcal{H}f$ is not defined for a non-integrable function like $f \sim |\eta|^{1/2}$.

Next, we shall consider the spatial structure of the flow in the interior of the fluid. Figure 4 shows the stream-function and the tangential vorticity in the (x, z) -plane for the initial condition and shortly before the singularity. While the structure of the stream function, an integral quantity of the flow, remains virtually unchanged, apart from a slight shift of the maximum towards $x = \pi$, the vorticity becomes strongly redistributed by the flow. The vorticity maxima approach each other and merge at the singularity time. The maxima of the vorticity at the free surface coincide with the maxima of the function $\partial_x \theta$ plotted in figure 3(c). Indeed, it can be shown using the definition $\hat{\omega} = ik\hat{V}_z - D\hat{V}_x$, the two-dimensional version of the continuity equation $ik\hat{V}_x = -D\hat{V}_z$ and the Stokes solution $\hat{V}_z = (\frac{1}{2}\hat{\theta}kz)\exp(kz)$ that $\hat{\omega}(z=0) = ik\hat{\theta}$ and thus the surface vorticity,

$$\omega(x, 0) = \partial_x \theta(x), \quad (3.42)$$

is identical to the derivative of the surfactant concentration.

Before proceeding to the two-dimensional case, we note parenthetically that the behaviour of an insoluble surfactant governed by

$$\partial_t \theta - \partial_x [(\mathcal{H}\theta)\theta] = 0, \quad (3.43)$$

is quite different from the behaviour of solutions to (3.40) since the mass $\int \theta dx$ is conserved in contrast to (3.40). For example, it can be shown (Thess 1996) that the width ℓ of a spreading insoluble surfactant distribution increases as $\ell \sim t^{1/2}$, while the corresponding soluble surfactant spreads as $\ell \sim t$. In general, the evolution of an insoluble surfactant proceeds slower since the conservation of mass inhibits surface renewal.

3.5. Dynamics of smooth surfactant distributions: the two-dimensional case

The two-dimensional evolution of a soluble surfactant, after rescaling of time by $t \rightarrow 2t$, is governed by the equation

$$\partial_t \theta - (\nabla \Delta^{-1/2} \theta) \cdot \nabla \theta = 0. \quad (3.44)$$

A similar equation, namely

$$\partial_t \theta - (\nabla_{\perp} \Delta^{-1/2} \theta) \cdot \nabla \theta = 0, \quad (3.45)$$

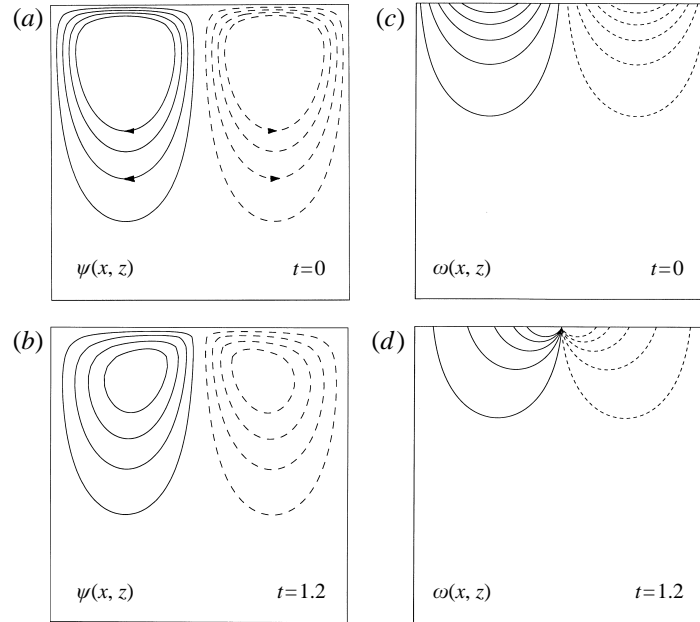


FIGURE 4. (a, b) Stream function and (c, d) tangential vorticity corresponding to the evolution shown in figure 3 plotted in the (x, z) -plane. (a, c) flow fields of the initial condition, (b, d) flow fields shortly before the singularity time $t_* = 1.275$. The flows are periodic in x with periodicity length 2π and extend from $z = 0$ to $z \rightarrow -\infty$. ψ and ω are related to the velocity field via $V_x = \partial_z \psi$, $V_y = -\partial_x \psi$, $\omega = \partial_x V_z - \partial_z V_x$.

with θ the potential temperature and $\nabla_{\perp} = \mathbf{e}_x \partial_y - \mathbf{e}_y \partial_x$ has been studied by Constantin *et al.* (1994a, b) as a model for geostrophic front formation. Moreover, it is worth mentioning that the two-dimensional Euler equation for the vorticity ω can be rewritten in the form

$$\partial_t \omega - (\nabla_{\perp} \Delta^{-1} \omega) \cdot \nabla \omega = 0. \tag{3.46}$$

The main difference between (3.45) and (3.46) on the one hand, and our equation (3.44) on the other hand, is that the velocity \mathbf{v} is perpendicular to the gradient of the scalar in the former cases, while it is parallel to the gradient in the latter case. As a result, the dynamics of our two-dimensional equation is locally very similar to the one-dimensional dynamics discussed in the previous section. Our two-dimensional simulations have shown that the velocity field induced by the non-uniform surfactant distribution leads to a steepening of the gradient $|\nabla \theta|$ and to a finite-time blow-up with the same characteristics as found in the one-dimensional case. Strictly speaking, the solution to (3.44) ceases to exist once a singularity has occurred at the ‘most dangerous’ point in the (x, y) -plane. For some initial conditions this singularity occurs almost immediately. In order to study the behaviour of near-singular structures for times beyond the singularity time, we have performed a simulation of (3.44) with a small phenomenological dissipative term $D \nabla^2 \theta$ added to the right-hand side that prevents the generation of arbitrarily small structures. Starting from the initial condition $\theta = \cos(2x) \cos(y) + \sin(x) \sin(y) + \cos(2x) \sin(3y)$ that has been used by Constantin *et al.* (1994b) for the investigation of (3.45) we observe a vigorous growth of the local maxima of θ , while the regions of minima get rapidly compressed. In the first stage of evolution extending approximately to $t \approx 0.7$, the growth of $|\nabla \theta|$ occurs most rapidly

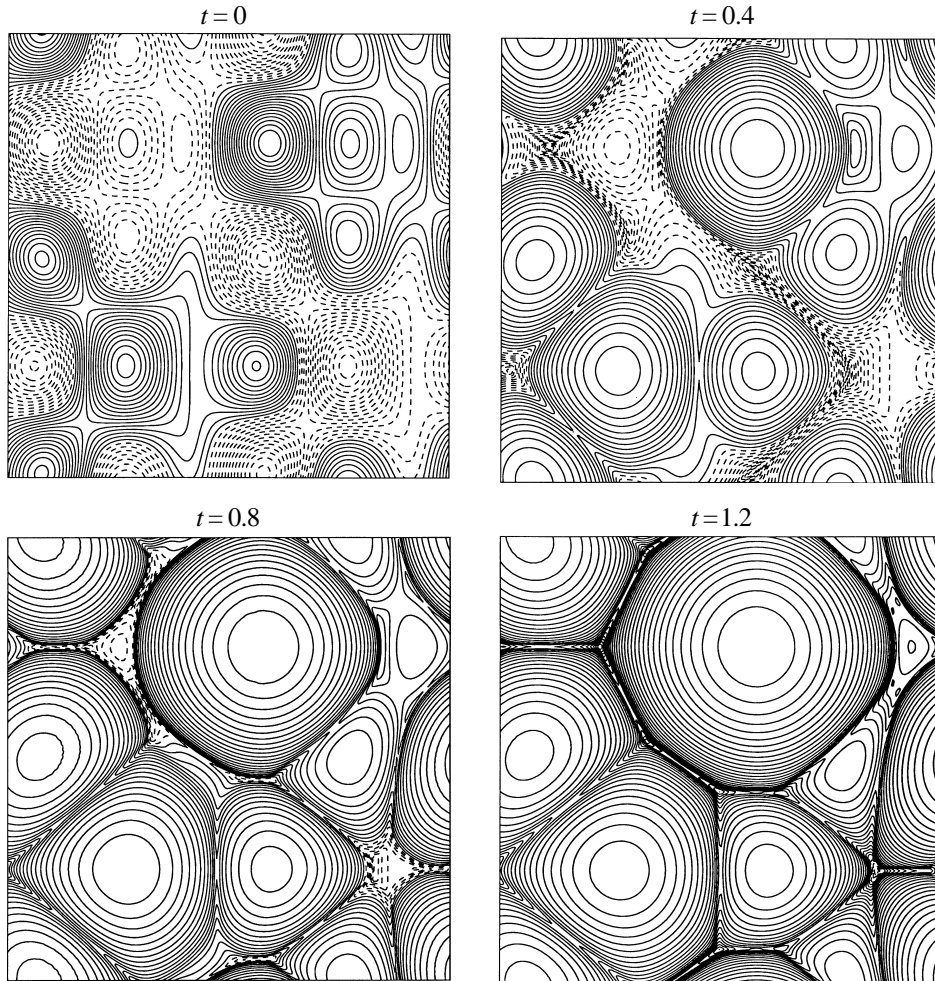


FIGURE 5. Formation of strong fronts in two-dimensional Marangoni convection. Surfactant concentration evolving from the initial condition $\theta = \cos(2x) \cos(y) + \sin(x) \sin(y) + \cos(2x) \sin(3y)$ obtained from a numerical solution of equation (3.44) with doubly periodic boundary conditions. Spatial resolution is 512×512 collocation points.

in the vicinity of the saddle points of the initial condition and leads to the formation of localized near-cusps. After this time the diffusive regularization prevents further steepening of $|\nabla\theta|$. In the second stage, the near-singular structures begin to spread in the transverse direction, forming straight singular fronts, which are clearly seen in the plots of figure 5 for $t = 0.8$ and $t = 1.2$. The spreading process comes to an end once the singular fronts have merged to form knots. We observe that the curvature of the function $\theta(x, y)$, which is proportional to $\nabla^2\theta$, forms strong maxima, almost delta functions, over the knots where in most cases three singular fronts merge. After the establishment of these strong spikes, the surfactant concentration homogenizes in a third stage, characterized by large timescales of the order D^{-1} .

The behaviour shown in figure 5 is in remarkably good agreement with full three-dimensional numerical simulations of the (thermal) Marangoni problem for high Marangoni numbers performed by Thess & Orszag (1995). This demonstrates

that the self-consistent model with the phenomenological dissipative term reproduces correctly the behaviour of the full three-dimensional problem and provides a rational framework to study strongly nonlinear Marangoni convection at greatly reduced computational expense.

It should be emphasized that the existence of a finite-time singularity in the non-diffusive model is not a deficiency of the theory but rather a signature of the strong energy transfer in wavenumber space. There are a few works (Cowley & Davis 1983; Zebib *et al.* 1985) that have demonstrated the possibility of sharp temperature gradients in the vicinity of walls in laterally heated Marangoni convection using boundary-layer analysis and numerical simulation. Our present theory shows that the existence of such structures, which become singular in the limit $Ma \rightarrow \infty$, does not necessarily require the presence of walls but represents an intrinsic property of the nonlinear advection process.

4. The effect of finite depth

An obvious generalization of the canonical problem follows from considering a layer with finite depth d . In the following two sections we shall derive the closure laws for a system with either no-slip boundary conditions or free-slip boundary conditions at the bottom. For convenience we shift the coordinate system such that the free surface is at $z = d$, and the bottom is at $z = 0$. Since the problem now has a natural lengthscale d , we use d , $\mu d/\Delta\sigma$, and $\Delta\theta$ as the scales for space, time and surfactant concentration. The Stokes problem for the functions $W(z) = \mu \hat{V}_z/\Delta\sigma$ and $H(z) = \mu d \hat{\Omega}_z/\Delta\sigma$ and the boundary conditions at the free surface $z = 1$ are the same as before, namely

$$(D^2 - k^2)^2 W = 0, \tag{4.1}$$

$$(D^2 - k^2)H = 0, \tag{4.2}$$

and

$$D^2 W(1) = -k^2 \hat{\theta}, \quad W(1) = 0, \quad DH(1) = 0. \tag{4.3}$$

4.1. Solution for the case when the bottom is a rigid boundary

The no-slip boundary condition $V = 0$ at $z = 0$ can be translated into the conditions

$$W(0) = 0, \quad DW(0) = 0, \quad H(0) = 0. \tag{4.4}$$

by using the continuity equation and the definition of the vertical vorticity (see also Chandasekhar 1961). As in §3, the equation for H decouples from the equation for W and since the boundary conditions for H are homogeneous, the only solution of (4.2), with $H(0) = DH(1) = 0$ is the trivial one $H = 0$. The fourth-order equation (4.1) for W has the general solution

$$W = c_1 e^{kz} + c_2 e^{-kz} + c_3 z e^{kz} + c_4 z e^{-kz}. \tag{4.5}$$

The four unknown coefficients are uniquely determined by the four boundary conditions. A straightforward calculation yields the result

$$W = \hat{\theta} \frac{k^2 \sinh(kz) - k^3 z \cosh(kz) + [k \coth(k) - 1] k^2 z \sinh(kz)}{k^2 \sinh(k) + k^3 \cosh(k) + [1 - k \cosh(k)] 2k \cosh(k) + k^2 \sinh(k)}, \tag{4.6}$$

for the vertical velocity from which, using the definitions (2.22) and (2.23), we deduce the closure law

$$\gamma_{\parallel}(k) = \frac{\sinh^2(k) - k^2}{k \sinh(2k) - 2k^2}, \quad \gamma_{\perp}(k) = 0. \quad (4.7)$$

Here, and in the following sections, we shall omit the subscript of γ_{\parallel} if γ_{\perp} is zero. The function $\gamma(k)$ is plotted in figure 6(a) together with that of the infinitely deep fluid, derived in the previous section. As expected, both closure laws become identical in the limit of large wavenumbers $k = 2\pi d/\ell$, since surfactant concentrations with periodicity length ℓ much smaller than d do not ‘feel’ the finite depth of the layer.

An interesting phenomenon occurs in the limit of small wavenumbers where $\gamma \rightarrow \frac{1}{4}$, as can be verified by performing a Taylor expansion of (4.7) around $k = 0$. In this case $\hat{\mathbf{v}} = -i\mathbf{k}\hat{\theta}/4$, which in physical space implies $\mathbf{v} = -\frac{1}{4}\nabla\theta$ and leads to the evolution equation

$$\partial_t\theta - \frac{1}{4}(\nabla\theta)^2 = 0 \quad (4.8)$$

for a soluble surfactant. After rescaling $\theta \rightarrow -4\theta$ this equation transforms into the well known two-dimensional Burgers equation

$$\partial_t\theta + (\nabla\theta)^2 = 0. \quad (4.9)$$

Thus, surface-tension driven flows with a characteristic lengthscale much larger than the depth of the layer are governed by the Burgers equation, which arises in other nonlinear extended systems as diverse as flame fronts (Sivashinsky 1983), the large-scale structure of the Universe (Vergassola *et al.* 1994), and dendritic growth (Kardar, Parisi & Zhang 1986).

4.2. Solution for the case when the bottom is a free boundary

For free-slip conditions $\Omega_x = \Omega_y = V_z = 0$, the procedure of §4.1 can be repeated with the boundary conditions (4.4) replaced by

$$W(0) = 0, \quad D^2W(0) = 0, \quad DH(0) = 0. \quad (4.10)$$

Again, the vertical vorticity vanishes for the same reasons as before, while the solution for W can be readily obtained as

$$W(z) = \hat{\theta} \frac{kz \sinh(k) \cosh(kz) - k \cosh(k) \sinh(kz)}{2 \sinh^2(k)}. \quad (4.11)$$

With this step done, we can evaluate the closure law as

$$\gamma_{\parallel}(k) = \frac{\sinh(2k) - 2k}{2k(\cosh(2k) - 1)}, \quad \gamma_{\perp}(k) = 0, \quad (4.12)$$

which is plotted in figure 6(b). The behaviour is qualitatively similar to the no-slip case. In the short-wave limit $k \rightarrow \infty$, the closure law becomes identical to that of the unbounded layer, while in the long-wave limit $k \rightarrow 0$, we obtain $\gamma \rightarrow \frac{1}{3}$. The larger value of γ in comparison with the no-slip case is due to the fact that a free-slip bottom provides less resistance to fluid motion than a no-slip bottom.

With the closure laws (4.7) and (4.12) the surface velocity can be formally represented as

$$\mathbf{v}(\mathbf{x}) = -\nabla \int G(\mathbf{x}' - \mathbf{x})\theta(\mathbf{x}')d^2\mathbf{x}', \quad (4.13)$$

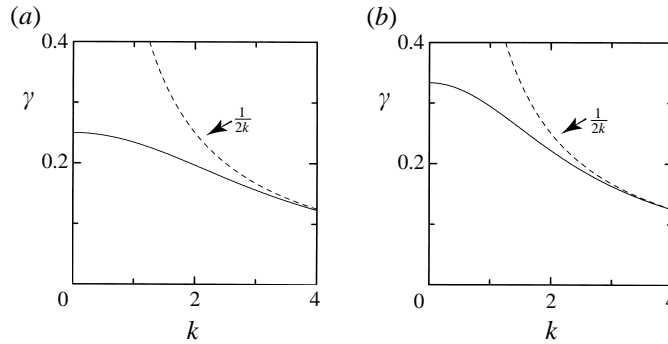


FIGURE 6. Closure law of a layer with finite depth with (a) no-slip condition (cf. (4.7)) and (b) with free-slip condition (cf. (4.12)) at the bottom. The wavenumber is made dimensionless with the layer depth d .

where the Green's function is

$$G(\mathbf{x}) = \frac{1}{4\pi} \int \gamma(k) e^{i\mathbf{k}\cdot\mathbf{x}} d^2\mathbf{k}. \tag{4.14}$$

However, we did not succeed in deriving an explicit analytic expression of the Green's function for either of the closure laws (4.7) or (4.12).

5. The effect of rotation

As a next step we consider a layer with infinite depth rotating with constant angular velocity Ω around the vertical axis. The rotation produces a Coriolis force

$$\mathbf{F} = -2\Omega \mathbf{e}_z \times \mathbf{V}, \tag{5.1}$$

which has to be taken into account when solving the Stokes problem (2.16)–(2.18). Two basic features of rotating Marangoni convection, however, can be understood without solving the Stokes problem. First, the presence of the Coriolis force entails a coupling between the vertical velocity and the vertical vorticity. As a result, radial surface flow is always accompanied by an azimuthal velocity component, rendering γ_{\perp} non-zero in contrast to the previous cases. Secondly, rotation induces a natural lengthscale into the problem, namely the thickness

$$\delta_E = \left(\frac{\nu}{2\Omega} \right)^{1/2} \tag{5.2}$$

of the Ekman boundary layer in the vicinity of the free surface. The Ekman layer represents the domain in rotating fluids where viscous forces and Coriolis forces are of comparable magnitude (Greenspan 1990). This lengthscale plays a similar role as the depth d in §4. Thus, in deriving the Stokes problem for the rotating system, it is natural to use the quantities δ_E , $\mu\delta_E/\Delta\sigma$, and $\Delta\theta$ as the scales for space, time and surfactant concentration. Inserting the Coriolis force (5.1) into (2.16) and (2.17) and using again $W(z) = \mu\hat{V}_z/\Delta\sigma$ and $H(z) = \mu\delta_E\hat{\Omega}_z/\Delta\sigma$ we obtain the Stokes equations in the form

$$(\mathbf{D}^2 - k^2)^2 W - \mathbf{D}H = 0, \tag{5.3}$$

$$(\mathbf{D}^2 - k^2)H + \mathbf{D}W = 0. \tag{5.4}$$

The boundary conditions at the free surface are as in the previous section

$$D^2W(0) = -k^2\hat{\theta}, \quad W(0) = 0, \quad DH(0) = 0, \quad (5.5)$$

as is the boundary condition $W \rightarrow 0$ and $H \rightarrow 0$ for $z \rightarrow -\infty$.

5.1. Solution for arbitrary wavenumber

First, we compute $W(z)$ by eliminating H . To this end we multiply (5.3) by $(D^2 - k^2)$, (5.4) with D , and add them in order to obtain

$$(D^2 - k^2)^3W + D^2W = 0 \quad (5.6)$$

as a single equation for W . The third boundary condition in (5.5) can be transformed into

$$(D^2 - k^2)^2W(0) = 0. \quad (5.7)$$

The general solution to (5.6) vanishing at $z \rightarrow -\infty$ is

$$W = c_1e^{q_1z} + c_2e^{q_2z} + c_3e^{q_3z}, \quad (5.8)$$

where the q_i are the roots of the cubic equation

$$(q^2 - k^2)^3 + q^2 = 0 \quad (5.9)$$

with positive real parts. The unknown coefficients c_i are uniquely determined by the first two boundary conditions in (5.5) and by (5.9). Once the c_i are determined, $H(z)$ can be computed as a solution of

$$(D^2 - k^2)H = -c_1q_1e^{q_1z} - c_2q_2e^{q_2z} - c_3q_3e^{q_3z}, \quad (5.10)$$

which can be written as

$$H(z) = -\frac{c_1q_1e^{q_1z}}{q_1^2 - k^2} - \frac{c_2q_2e^{q_2z}}{q_2^2 - k^2} - \frac{c_3q_3e^{q_3z}}{q_3^2 - k^2} + c_4e^{kz}. \quad (5.11)$$

The coefficient c_4 is obtained by enforcing the boundary condition (5.5).

A lengthy but straightforward computation of the coefficients c_1 to c_4 leads, on using the definitions (2.22) and (2.23), to the following closure laws for the rotating layer

$$\gamma_{\parallel}(k) = \frac{(q_1^2 - k^2)^2(q_2 - q_3) + (q_2^2 - k^2)^2(q_3 - q_1) + (q_3^2 - k^2)^2(q_1 - q_2)}{q_1^4(q_2^2 - q_3^2) + q_2^4(q_3^2 - q_1^2) + q_3^4(q_1^2 - q_2^2)}, \quad (5.12)$$

$$\gamma_{\perp}(k) = \frac{\frac{(q_3^2 - k^2)^2 - (q_2^2 - k^2)^2}{k(1 + kq_1^{-1})} + \frac{(q_1^2 - k^2)^2 - (q_3^2 - k^2)^2}{k(1 + kq_2^{-1})} + \frac{(q_2^2 - k^2)^2 - (q_1^2 - k^2)^2}{k(1 + kq_3^{-1})}}{q_1^4(q_2^2 - q_3^2) + q_2^4(q_3^2 - q_1^2) + q_3^4(q_1^2 - q_2^2)}, \quad (5.13)$$

plotted in figure 7. We have verified by using symbolic computation, that both γ_{\parallel} and γ_{\perp} are real functions even though the roots q_i are in general complex. The reader is urged not to be intimidated by the apparent complexity of these equations, the detailed structure of which is not essential to the understanding of their physical content.

Figure 7(a) shows that the behaviour of the parallel velocity component in rotating convection strongly resembles that of convection in a non-rotating finite sheet plotted in figure 6. In the short-wave limit $k \rightarrow \infty$, when the lengthscale of surfactant concentration variations is much smaller than the thickness of the Ekman layer, γ_{\parallel}

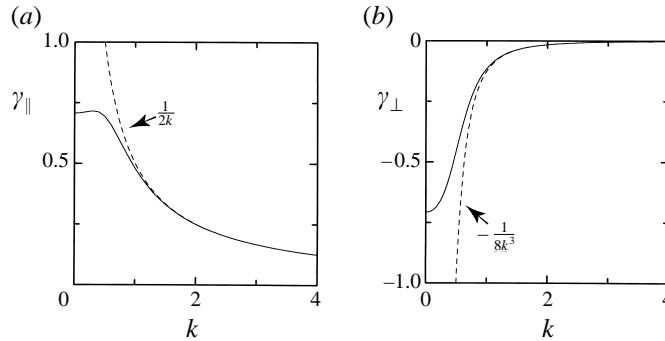


FIGURE 7. Closure law for (a) the longitudinal (cf. (5.12)) and (b) for the transverse (cf. (5.13)) velocity components in a rotating layer with infinite depth. The wavenumber is made dimensionless with the thickness of the Ekman boundary layer $\delta_E = (\nu/2\Omega)^{1/2}$.

k	$\gamma_{\parallel}(k)$	$\gamma_{\perp}(k)$
0	7.071×10^{-1}	-7.071×10^{-1}
0.2	7.130×10^{-1}	-6.751×10^{-1}
0.4	7.121×10^{-1}	-5.497×10^{-1}
0.6	6.598×10^{-1}	-3.539×10^{-1}
0.8	5.675×10^{-1}	-2.005×10^{-1}
1.0	4.787×10^{-1}	-1.145×10^{-1}
2.0	2.492×10^{-1}	-1.553×10^{-2}
3.0	1.665×10^{-1}	-4.624×10^{-3}
4.0	1.249×10^{-1}	-1.952×10^{-3}

TABLE 2. Numerical values of the closure law for surface-tension driven convection in a rotating layer with infinite depth (equations (5.12) and (5.13))

becomes identical to that of the unbounded layer. The transverse velocity component decays much faster for large k than the longitudinal velocity. This will be explained in connection with the asymptotic theory for $k \rightarrow \infty$, to be developed below. From the negative sign of γ_{\perp} we can conclude that for a layer rotating anticlockwise, the trajectory of a particle flowing in the direction opposite to the gradient $\nabla\theta$ is deflected to the right, as is to be expected of flows under the influence of a Coriolis force.

In the short-wave limit $k \rightarrow 0$, which corresponds to structures much larger than the Ekman-layer thickness, both functions tend to constant values $\gamma_{\parallel} = 1/\sqrt{2} \approx 0.707$ and $\gamma_{\perp} = -1/\sqrt{2}$. Consequently, in a fluid rotating in the positive sense, the velocity of large-scale perturbations has turned 45° to the right of the velocity in a non-rotating layer. This phenomenon is reminiscent of the behaviour of the ordinary Ekman layer in geophysical flows (see e.g. Pedlosky 1987). Selected numerical values of γ_{\parallel} and γ_{\perp} are listed in table 2. In the next sections we analyse the limiting cases of large and small wavenumbers.

5.2. Asymptotic solution for $k \gg 1$

In order to solve the Stokes problem (5.3)–(5.5) for $k \gg 1$ we introduce the small parameter $\epsilon = k^{-1}$ and the new variables $\zeta = kz$, $D_{\zeta} = d/d\zeta$, $S = k^2W$. In terms of the new variables the Stokes problem transforms into

$$(D_{\zeta}^2 - 1)^2S - \epsilon D_{\zeta}H = 0, \tag{5.14}$$

$$(D_\zeta^2 - 1)H + \epsilon^3 D_\zeta S = 0, \quad (5.15)$$

with the boundary conditions

$$D_\zeta^2 S(0) = 1, \quad S(0) = 0, \quad D_\zeta H(0) = 0. \quad (5.16)$$

We seek the asymptotic solutions for S and H as a power series in the form

$$S(\zeta) = \epsilon^0 S_0 + \epsilon^1 S_1 + \epsilon^2 S_2 + \epsilon^3 S_3 + O(\epsilon^4), \quad (5.17)$$

$$H(\zeta) = \epsilon^0 H_0 + \epsilon^1 H_1 + \epsilon^2 H_2 + \epsilon^3 H_3 + O(\epsilon^4). \quad (5.18)$$

Inserting this ansatz into (5.14)–(5.16) and equating the coefficients for each power of ϵ , we obtain a chain of equations determining the functions S_i and H_i . To zero order in ϵ we have the equations and boundary conditions

$$(D_\zeta^2 - 1)^2 S_0 = 0, \quad (5.19)$$

$$(D_\zeta^2 - 1)H_0 = 0, \quad (5.20)$$

$$S_0(0) = D_\zeta^2 S_0(0) - 1 = D_\zeta H_0(0) = 0. \quad (5.21)$$

which are identical to those for the unbounded layer with $k = 1$ and have the solutions

$$S_0 = \frac{1}{2} \zeta e^\zeta, \quad H_0 = 0. \quad (5.22)$$

The first- and second-order equations and boundary conditions are both of the form

$$(D_\zeta^2 - 1)^2 S_n - D_\zeta H_n = 0, \quad (5.23)$$

$$(D_\zeta^2 - 1)H_n = 0, \quad (5.24)$$

$$S_n(0) = D_\zeta^2 S_n(0) = D_\zeta H_n(0) = 0, \quad (5.25)$$

where $n = 1$ or $n = 2$. Since both the equations and the boundary conditions are homogeneous and linear, the only solution is the trivial one $S_n = H_n = 0$ for $n = 1, 2$. The third-order problem reads

$$(D_\zeta^2 - 1)^2 S_3 - D_\zeta H_3 = 0, \quad (5.26)$$

$$(D_\zeta^2 - 1)H_3 + D_\zeta S_0 = 0, \quad (5.27)$$

$$S_3(0) = D_\zeta^2 S_3(0) = D_\zeta H_3(0) = 0. \quad (5.28)$$

The solution

$$S_3 = 0, \quad H_3 = \frac{1}{8}(1 - \zeta - \zeta^2)e^\zeta, \quad (5.29)$$

together with (5.22) provides the desired analytic expressions

$$\gamma_\parallel(k) = \frac{1}{2k}, \quad \gamma_\perp(k) = -\frac{1}{8k^3}, \quad (5.30)$$

for the leading-order asymptotic terms of the closure law for the rotating layer. The curves are plotted as dashed lines in figure 7. It follows from (5.30) that the ratio between the transverse and longitudinal velocity components decreases with increasing wavenumber as $v_\perp/v_\parallel = \gamma_\perp/\gamma_\parallel \sim k^{-2} \sim (\ell^2/\delta_E^2) \sim \ell^2\Omega/\nu$ where ℓ denotes the spatial periodicity length of θ . A simple physical interpretation of this phenomenon can be given by estimating the magnitude of the perpendicular velocity component v_\perp from the longitudinal velocity v_\parallel using the balance between viscous forces and the Coriolis force, expressed by the Stokes equation (2.11). This equation implies

$$\nu \nabla^2 v_\perp \sim \Omega v_\parallel. \quad (5.31)$$

Since $\ell \ll \delta_E$, the Laplacian can be estimated as $\nabla^2 \sim \ell^{-2}$, and we obtain $v_{\perp} \sim (\ell^2 \Omega / \nu) v_{\parallel}$ which is exactly the desired relation.

5.3. Asymptotic solution for $k \ll 1$

In the limit $k \ll 1$, the structures are much larger than the depth of the Ekman layer. Using (5.6) as a starting point, we obtain

$$(D^6 + D^2)W = 0, \tag{5.32}$$

with the boundary conditions (5.5) as the zero-order equation for W . Of the six zeros of the characteristic equation $\lambda^6 + \lambda^2 = 0$, only two, namely $\lambda_{1/2} = (1 \pm i)/\sqrt{2}$, have a positive real part. Therefore the solution of (5.31), which decays at infinity, must have the form

$$W = c_1 e^{\lambda_{1z}} + c_2 e^{\lambda_{2z}}. \tag{5.33}$$

To leading order in k^2 the first two boundary conditions in (5.5) are satisfied if $c_1 = -c_2$, while (5.7) requires $i(c_1 - c_2) = -k^2 \hat{\theta}$. As a result, the solution for W takes the form

$$W = -k^2 \hat{\theta} \exp\left(\frac{z}{\sqrt{2}}\right) \sin\left(\frac{z}{\sqrt{2}}\right). \tag{5.34}$$

From the knowledge of W the function H is readily obtained by solving the leading-order equation

$$D^2 H + D W = 0 \tag{5.35}$$

with the third boundary condition (5.5). The result

$$H = \frac{1}{\sqrt{2}} k^2 \hat{\theta} \exp\left(\frac{z}{\sqrt{2}}\right) \left[\sin\left(\frac{z}{\sqrt{2}}\right) - \cos\left(\frac{z}{\sqrt{2}}\right) \right] \tag{5.36}$$

together with (5.34) immediately furnishes the asymptotic expressions

$$\gamma_{\parallel}(k) = \frac{1}{\sqrt{2}}, \quad \gamma_{\perp}(k) = -\frac{1}{\sqrt{2}}, \tag{5.37}$$

for the closure law of a rotating layer in the long-wave limit.

The physical meaning of these relations can be understood using the same arguments as in the previous section with the estimate for the action of the Laplacian replaced by $\nabla^2 \sim \delta_E^{-2}$, which is the consequence of the fact that the Ekman-layer thickness is now the dominant scale of the problem. The estimate $v_{\perp} \sim (\delta_E^2 \Omega / \nu) v_{\parallel} \sim v_{\parallel}$ is consistent with (5.37).

Linear Marangoni instability in rotating fluids has been studied by Namikawa, Takashima & Matsushita (1970). The present formulation, in particular (2.12) with (5.12) and (5.13), provides the strongly nonlinear counterpart to the linear stability approach.

6. The effect of a magnetic field

Consider a layer of electrically conducting fluid subjected to a homogeneous vertical magnetic field $B_0 \mathbf{e}_z$. The interaction between the Marangoni convection and the magnetic field leads to the induction of electric currents which, by virtue of Joule dissipation, reinforce the dissipative action of ordinary viscosity. Magnetic control of free-surface flows is important in various materials' processing technologies.

The action of the magnetic field upon the fluid is described by the Lorentz force per unit mass

$$\mathbf{F} = \frac{1}{\rho\mu_0}(\tilde{\nabla} \times \mathbf{B}) \times \mathbf{B} \quad (6.1)$$

which has to be inserted into the Stokes equation (2.18) and (2.19). In general, the magnetic field must be determined by solving the equations

$$\partial_t \mathbf{B} + (\mathbf{V} \cdot \tilde{\nabla}) \mathbf{B} = (\mathbf{B} \cdot \tilde{\nabla}) \mathbf{V} + \frac{1}{\sigma_{el}\mu_0} \tilde{\nabla}^2 \mathbf{B}, \quad (6.2)$$

$$\tilde{\nabla} \cdot \mathbf{B} = 0. \quad (6.3)$$

The derivation of these equations from Maxwell's equations and Ohm's law can be found in standard textbooks on magnetohydrodynamics (e.g. Moreau 1990). Here μ_0 and σ_{el} denote the magnetic permeability and the electrical conductivity of the fluid, respectively. We are interested in a situation where the magnetic field perturbation induced by the fluid motion is much weaker than the applied magnetic field. This condition is fulfilled if the magnetic Reynolds number $Rm = \mu_0\sigma_{el}\ell v$ with ℓ a characteristic lengthscale and v a characteristic velocity of the motion is very small, as is the case for most laboratory experiments and industrial applications. The assumption $Rm \ll 1$ permits us to write the magnetic field as

$$\mathbf{B} = B_0 \mathbf{e}_z + \mathbf{B}' \quad (6.4)$$

and to linearize the magnetic field equation with respect to \mathbf{B}' . Moreover, for liquid metals the magnetic Prandtl number $Pm = \nu\sigma_{el}\mu_0$ is very small, expressing the fact that the relaxation of the magnetic field occurs much faster than viscous relaxation. Therefore, we can neglect the time-derivative of the magnetic field too. We are left with the equation

$$\tilde{\nabla}^2 \mathbf{B}' + B_0\mu_0\sigma_{el}\partial_z \mathbf{V} = 0 \quad (6.5)$$

for the magnetic field perturbation. Neglecting quadratic terms in the magnetic field perturbation the Lorentz force can be expressed as

$$\mathbf{F} = \frac{B_0}{\rho\mu_0} (\partial_z \mathbf{B}' - \tilde{\nabla} B'_z). \quad (6.6)$$

Based on relations (6.5) and (6.6) and the Stokes equation (2.16) and (2.17) we can derive the following equations for the vertical velocity, vertical vorticity, and vertical component of magnetic field perturbation in Fourier space

$$\nu(D^2 - k^2)^2 \hat{V}_z - \frac{B_0}{\rho\mu_0} D(D^2 - k^2) \hat{B}'_z = 0, \quad (6.7)$$

$$\nu(D^2 - k^2) \hat{\Omega}_z = 0, \quad (6.8)$$

$$\frac{1}{\sigma_{el}\mu_0} (D^2 - k^2) \hat{B}'_z + B_0 D \hat{V}_z = 0. \quad (6.9)$$

The magnetic field can be eliminated from the stability problem by inserting (6.9) into (6.7) which leads to

$$(D^2 - k^2)^2 \hat{V}_z + \left(\frac{B_0^2 \sigma_{el}}{\rho\nu} \right) \partial_z^2 \hat{V}_z = 0. \quad (6.10)$$

Flows of electrically conducting fluids in the presence of a magnetic field are characterized by the existence of a Hartmann boundary layer with thickness

$$\delta_H = \frac{1}{B_0} \left(\frac{\mu}{\sigma_{el}} \right)^{1/2}, \tag{6.11}$$

which provides a natural lengthscale for the problem at hand. Within the Hartmann layer the viscous forces and the electromagnetic forces are of the same order of magnitude. Based on this, we use the quantities δ_H , $\mu\delta_H/\Delta\sigma$, and $\Delta\theta$ as the scales for space, time and surfactant concentration. Introducing as in previous sections the functions $W(z) = \mu\hat{V}_z/\Delta\sigma$ and $H(z) = \mu\delta_H\hat{\Omega}_z/\Delta\sigma$ we obtain the Stokes equations in the form

$$(D^2 - k^2)^2 W - D^2 W = 0, \tag{6.12}$$

$$(D^2 - k^2)H = 0. \tag{6.13}$$

The boundary conditions at the free surface are

$$D^2 W(0) = -k^2\hat{\theta}, \quad W(0) = 0, \quad DH(0) = 0. \tag{6.14}$$

The reader interested in the details of the derivation of the magnetic Stokes problem is referred to Chandrasekhar's (1961) classical textbook. With the positive roots

$$q_{1/2} = \frac{1}{2} \left((1 + 4k^2)^{1/2} \pm 1 \right) \tag{6.15}$$

of the characteristic equation $(q^2 - k^2)^2 - q^2 = 0$ we can express the solution of (6.12) as

$$W = c_1 e^{q_{1z}} + c_2 e^{q_{2z}}. \tag{6.16}$$

Enforcing the boundary conditions gives the result

$$W = -\frac{k^2\hat{\theta}}{(1 + 4k^2)^{1/2}} (e^{q_{1z}} - e^{q_{2z}}) \tag{6.17}$$

and the closure law

$$\gamma_{\parallel}(k) = \frac{1}{(1 + 4k^2)^{1/2}}, \quad \gamma_{\perp}(k) = 0 \tag{6.18}$$

which is plotted in figure 8.

It becomes evident by inspection of figure 8 that the behaviour of convection in an infinite layer in the presence of a magnetic field is similar to convection in a layer with finite depth where the Hartmann boundary-layer thickness plays the role of the depth. For perturbations with periodicity length much smaller than δ_H the closure law is identical to that of the unbounded layer. For large-scale perturbations the role of the Hartmann boundary layer consists in confining the flow to the immediate vicinity of the free surface. Thus in the limit $k \rightarrow 0$ we have $\gamma \rightarrow \frac{1}{2}$ which implies that large-scale perturbations are governed by the Burgers equation.

7. Summary and conclusions

We have investigated surface tension driven flows set up by a scalar with zero diffusivity. The main result of the work consists of a systematic derivation of closure laws, relating the surface velocity field to the distribution of the surface tension at the free surface. These closure laws are summarized in table 3 together with their asymptotic behaviour for large and small wavenumber. In conjunction with

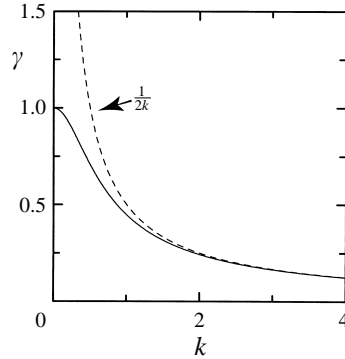


FIGURE 8. Closure law of a layer with infinite depth subject to a vertical magnetic field (cf. (6.18)). The wavenumber is made dimensionless with the thickness of the Hartmann boundary layer $\delta_H = (\mu/\sigma_{el})^{1/2}/B$.

System	Exact relation	$k \ll 1$	$k \gg 1$
Semi-infinite layer	$\gamma_{\parallel} = \frac{1}{2k}$	$\gamma_{\parallel} = \frac{1}{2k}$	$\gamma_{\parallel} = \frac{1}{2k}$
Finite layer with rigid lower boundary	$\gamma_{\parallel} = \frac{\sinh^2(k) - k^2}{k \sinh(2k) - 2k^2}$	$\gamma_{\parallel} = \frac{1}{4}$	$\gamma_{\parallel} = \frac{1}{2k}$
Finite layer with free lower boundary	$\gamma_{\parallel} = \frac{\sinh^2(k) - 2k}{2k \cosh(2k) - 2k}$	$\gamma_{\parallel} = \frac{1}{3}$	$\gamma_{\parallel} = \frac{1}{2k}$
Rotating semi-infinite layer	γ_{\parallel} : equation (5.12)	$\gamma_{\parallel} = \frac{1}{\sqrt{2}}$	$\gamma_{\parallel} = \frac{1}{2k}$
	γ_{\perp} : equation (5.13)	$\gamma_{\perp} = -\frac{1}{\sqrt{2}}$	$\gamma_{\perp} = -\frac{1}{8k^3}$
Semi-infinite layer with vertical magnetic field	$\gamma_{\parallel} = \frac{1}{(1 + 4k^2)^{1/2}}$	$\gamma_{\parallel} = 1$	$\gamma_{\parallel} = \frac{1}{2k}$

TABLE 3. Summary of closure laws obtained in the present work. $\gamma_{\perp} = 0$ in all cases where only γ_{\parallel} is given.

equations (2.12) and (2.13) the closure laws lead to self-consistent two-dimensional models of Marangoni convection that are not only useful in analysing nonlinear self-organization and pattern formation but are also of mathematical interest in their own right. The present theory is derived for zero Reynolds number, implying that the application of the theory to real problems is bounded from above by the requirement that the inertia does not significantly affect the dynamics of the flow. It would be interesting to generalize the model to the finite-Reynolds-number case using perturbation theory.

The examples treated in the present work have not been chosen at random. Apart from the infinitely deep layer, they are all characterized by a single lengthscale. Using this length as a characteristic scale, the closure laws and the evolution equations can be written in a universal non-dimensional form that is free of any parameters such as Ekman number or Hartmann number. Any further generalization of the models, such as rotating convection in a finite layer, convection in a two-layer system, convection under the combined influence of rotation and magnetic field or

convection driven by more than one scalar field would require the introduction of non-dimensional parameters and render the closure laws more complicated. Apart from this technical aspect, however, such generalizations are deemed useful for improving our understanding of Marangoni convection. Moreover, it would be interesting to use the equations as a model for chemical Marangoni convection, thereby extending the linear and weakly nonlinear stability studies of Rabinovich, Vyazmin & Buyevich (1993, 1995) into the strongly nonlinear regime. This could be accomplished by writing down equations analogous to (2.12) for the concentration of each species and adding to the right-hand side appropriate terms accounting for the reaction kinetics.

A similar approach can be taken in order to model the general surfactant dynamics, characterized by the presence of both bulk concentration C (with the value c at the free surface) and excess surface concentration c_s as already mentioned in §2. Under the assumption that the bulk-diffusivity is zero, the system is governed by the two-dimensional model

$$\partial_t c + (\mathbf{v}[c_s] \cdot \nabla)c = 0, \quad (7.1)$$

$$\partial_t c_s + \nabla \cdot (\mathbf{v}[c_s]c_s) = D_s \nabla^2 c_s + J(c_s, c). \quad (7.2)$$

Once the transport relation J is specified, this set of equations becomes a self-consistent model. The lack of a vertical diffusive flux of surfactant can be overcome by adding a phenomenological source term to (7.1).

Our results for the rotating case may find applications in geophysical fluid dynamics for phenomenological modelling of thermohaline convection (Whitehead 1995). Since the thickness of the thermocline is usually much less than the depth of the ocean, it may be, to a first approximation, regarded as a thin film governed by (2.13) with closure (2.12) and (2.13).

The present theory can be generalized in a straightforward manner to curved interfaces. This is important for application in chemical engineering, where spherical bubbles or drops are often encountered. From the theoretical perspective it would be desirable to perform a detailed investigation of the mathematical structure of the finite-time singularities, at which we have provided only a first glimpse. Finally, by adding a phenomenological random-force-term describing 'energy injection' the insoluble surfactant equation

$$\partial_t \theta + \nabla(\mathbf{v} \cdot \theta) = D \nabla^2 \theta + f(\mathbf{x}, t), \quad (7.3)$$

could be used as a simplified model for interfacial turbulence in high-Schmidt-number problems or high-Prandtl-number fluids.

Note added in proof. P. Colinet (1996, personal communication) uses an instability term instead of random force in order to drive the system.

We are grateful to Th. Boeck, A. Golovin, K. Nitschke, R. Picard, L. Pismen and M. Romero for useful comments and discussions. An anonymous referee is acknowledged for his constructive criticism. This work has been partially supported by the Deutsche Forschungsgemeinschaft.

REFERENCES

- AREF, H. 1983 *Ann. Rev. Fluid Mech.*, **15**, 345–389.
 BERG, J. C., ACRIVOS, A. & BOUDART, M. 1966 *Evaporative Convection, Advances in Chemical Engineering*, vol. 6, pp. 61–123. Academic.

- CHANDRASEKHAR, S. 1961 *Hydrodynamic and Hydromagnetic Stability*. Oxford University Press.
- CONSTANTIN, P., MAJDA, A. & TABAK, E. 1994a *Phys. Fluids* **6**, 9–11.
- CONSTANTIN, P., MAJDA, A. & TABAK, E. 1994b *Nonlinearity* **7**, 1495–1533.
- COWLEY, S. J. & DAVIS, S. H. 1983 *J. Fluid Mech.* **135**, 175–188.
- DAVIS, S. H. 1987 *Ann. Rev. Fluid Mech.* **19**, 347–359.
- DEWIT, A., GALLEZ, D. & CHRISTOV, C. I. 1994 *Phys. Fluids* **6**, 3256–3266.
- EDWARDS, D. A., BRENNER, H. & WASAN, D. T. 1991 *Interfacial Transport Processes and Rheology*. Butterworth–Heinemann.
- EGGERS, J. 1993 *Phys. Rev. Lett.* **71**, 3458–3460.
- ERDÉLYI, A. 1954 *Tables of Integral Transforms*. McGraw Hill.
- GOLDSTEIN, R., PESCI, A. I. & SHELLEY, M. J. 1995 *Phys. Rev. Lett.* **75**, 3665–3668.
- GRAUER, R. & SIDERIS, T. C. 1995 *Physica D* **88**, 116–132.
- GREENSPAN, H. P. 1990 *The Theory of Rotating Fluids*. Breukelen Press.
- GROTBERG, J. B. 1994 *Ann. Rev. Fluid Mech.* **26**, 529–571.
- HELGAßON, S. 1980 *The Radon Transform, Progress in Mathematics* **5**, Birkhäuser.
- JANSON, K. M. & LISTER, J. R. 1988 *Phys. Fluids* **31**, 1321–1323.
- JENSEN, O. E. 1995 *J. Fluid Mech.* **293**, 349–378.
- JENSEN, O. E. & GROTBERG, J. B. 1992 *J. Fluid Mech.* **240**, 259–288.
- JENSEN, O. E. & GROTBERG, J. B. 1993 *Phys. Fluids A* **5**, 58–68.
- KARDAR, M., PARISI, G. & ZHANG, Y. C. 1986 *Phys. Rev. Lett.* **56**, 889–892.
- KOSCHMIEDER, E. L. 1993 *Bénard Cells and Taylor Vortices*. Cambridge University Press.
- KUZNETSOV, M. D., SPECTOR, M. & ZAKHAROV, V. E. 1994 *Phys. Rev. E* **49**, 1283–1290.
- LANDAU, L. D. & LIFSHITZ, E. M. 1987 *Fluid Mechanics, Course of Theoretical Physics*, **6**. Pergamon Press.
- LEVICH, V. G. 1962 *Physicochemical Hydrodynamics*, Prentice Hall.
- LUBENSKY, D. K. & GOLDSTEIN, R. E. 1996 *Phys. Fluids* **8**, 843–854.
- MOREAU, R. 1990 *Magnetohydrodynamics*. Kluwer.
- NAMIKAWA, T., TAKASHIMA, M. & MATSUSHITA, S. 1970 *J. Phys. Soc. Japan* **28**, 1340–1349.
- NITSCHKE, K. & THESS, A. 1995 *Phys. Rev. E* **52**, R5772–R5775.
- OLIVER, D. L. R. & DE WITT, K. J. 1994 *J. Colloid Interface Sci.* **164**, 263–268.
- ORON, A. & ROSENAU, P. 1994 *J. Fluid Mech.* **273**, 361–374.
- PARK, C. W., MARUVADA, S. R. K. & YOON, D. Y. 1994 *Phys. Fluids* **6**, 3267–3275.
- PEDLOSKY, J. 1987 *Geophysical Fluid Dynamics*. Springer.
- POZRIKIDIS, C. 1992 *Boundary Integral and Singularity Methods for Linearized Viscous Flow*. Cambridge University Press.
- PUMIR, A. & SIGGIA, E. 1992 *Phys. Rev. Lett.* **68**, 1511–1514.
- RABINOVICH, L. M., VYAZMIN, A. V. & BUYEVICH, YU. A. 1993 *J. Colloid Interface Sci.* **157**, 202–218.
- RABINOVICH, L. M., VYAZMIN, A. V. & BUYEVICH, YU. A. 1995 *J. Colloid Interface Sci.* **173**, 1–7.
- SARPKAYA, T. 1996 *Ann. Rev. Fluid Mech.* **28**, 83–128.
- SCRIVEN, L. & STERNLING, C. 1964 *J. Fluid Mech.* **21**, 321–340.
- SIVASHINSKY, G. I. 1983 *Ann. Rev. Fluid Mech.* **15**, 179–199.
- THESS, A. 1996 *Physica Scripta*, to appear.
- THESS, A. & ORSZAG, S. A. 1995 *J. Fluid Mech.* **283**, 201–230.
- THESS, A., SPIRN, D. & JÜTTNER, B. 1995 *Phys. Rev. Lett.* **75**, 4614–4617.
- TRYGGVASON, G., ABDOLLAHI-ALIBEIK, J., WILMARTH, W. W. & HIRSA, A. 1992 *Phys. Fluids A* **4**, 1215–1229.
- TSAI, W. T. & YUE D. K. P. 1995 *J. Fluid Mech.* **289**, 315–349.
- TURING, A. M. 1952 *Phil. Trans. R. Soc. Lond. B* **237**, 37.
- VERGASSOLA, M., DUBRULLE, B., FRISCH, U. & NOULLEZ, A. 1994 *Astron. Astrophys.* **298**, 325–356.
- WHITEHEAD, J. A. 1995 *Ann. Rev. Fluid Mech.* **27**, 89–113.
- ZEBIB, A., HOMSY, G. M. & MEIBURG, E. 1985 *Phys. Fluids* **28**, 3467–3476.